Cestode larvae excite host neuronal circuits via glutamatergic signaling.

Anja de Lange[*1,2,3], Hayley Tomes[*1,2,3], Joshua Selfe[1,2,3], Ulrich Fabien Prodjinotho[4], Matthijs Bernard Verhoog[1,2], Siddhartha Mahanty[5], Katherine Smith[3,6], William Horsnell[3,7,8], Chummy Sikasunge[9], Clarissa Prazeres da Costa[4], Joseph Valentino Raimondo[1,2,3]

[*]Authors contributed equally

[1]Division of Cell Biology, Department of Human Biology, Neuroscience Institute, Faculty of Health Sciences, University of Cape Town, Cape Town, South Africa
[2]Neuroscience Institute, Faculty of Health Sciences, University of Cape Town, Cape Town, South Africa
[3]Institute of Infectious Disease and Molecular Medicine, Faculty of Health Sciences, University of Cape Town, Cape Town, South Africa
[4]Center for Global Health, TUM School of Medicine, Technical University of Munich (TUM), Munich, Germany
[5]Department of Medicine, The Peter Doherty Institute for Infection and Immunity and the Victorian Infectious Diseases Service, University of Melbourne, Melbourne, Australia
[6]School of Biosciences, Cardiff University, Cardiff, United Kingdom
[7]Institute of Microbiology and Infection, University of Birmingham, Birmingham, United Kingdom
[8]Laboratory of Experimental and Molecular Immunology and Neurogenetics (INEM), UMR 7355 CNRS-University of Orleans, Orleans, France
[9]School of Veterinary Medicine, Department of Paraclinicals, University of Zambia, Lusaka, Zambia

Correspondence:
Joseph V. Raimondo
email: joseph.raimondo@uct.ac.za

Keywords
Cestode, *Taenia crassiceps*, *Taenia solium*, neurocysticercosis, glutamate, aspartate, seizures

Abstract
Neurocysticercosis (NCC) is caused by infection of the brain by larvae of the parasitic cestode *Taenia solium*. It is the most prevalent parasitic infection of the central nervous system and one of the leading causes of adult-acquired epilepsy worldwide. However, little is known about how cestode larvae affect neurons directly. To address this, we used whole-cell patch-clamp electrophysiology and calcium imaging in rodent and human brain slices to identify direct effects of cestode larval products on neuronal activity. We found that both whole cyst homogenate and excretory/secretory products of cestode larvae have an acute excitatory effect on neurons, which can trigger seizure-like events *in vitro*. Underlying this effect was cestode-induced neuronal depolarization, which was mediated by

glutamate receptor activation but not by nicotinic acetylcholine receptors, acid-sensing ion channels nor Substance P. Glutamate-sensing fluorescent reporters (iGluSnFR) and amino acid assays revealed that the larval homogenate of the cestodes *Taenia crassiceps* and *Taenia solium* contained high concentrations of the amino acid's glutamate and aspartate. Furthermore, we found that larvae of both species consistently produce and release these excitatory amino acids into their immediate environment. Our findings suggest that perturbations in glutamatergic signaling may play a role in seizure generation in NCC.

51 *Introduction*

52 Neurocysticercosis (NCC) is the most prevalent parasitic infection of the central nervous system (CNS)
53 (1,2). It is caused by the presence of larvae of the cestode *Taenia solium (T. solium)* in the brain (3).
54 The most common symptom of NCC is recurrent seizures (4). As a result, NCC is one of the leading
55 causes of adult-acquired epilepsy worldwide (5), resulting in significant morbidity and mortality. In
56 *T.solium* endemic areas, 29% of people with epilepsy also had NCC (6). Despite the impact of NCC,
57 there are a paucity of studies investigating the seizure mechanisms involved (7). As far as we are
58 aware, to date there have been no studies investigating the direct, acute effects of cestode larval
59 products on neurons. As a result, precisely how larvae perturb neuronal circuits is still relatively poorly
60 understood.

61

62 In NCC seizures may occur at any stage following initial infection (8). It is thought that inflammatory
63 processes in the brain play an important role in the development of recurrent seizures (9). Previous
64 research investigating seizure development in NCC has therefore typically focused on how the host
65 neuroinflammatory response to larvae might precipitate seizures (7,10). One study by Robinson *et al*.
66 found that production of the inflammatory molecule and neurotransmitter, Substance P, produced by
67 peritoneal larval granulomas, precipitated acute seizures (11). In addition to host-derived substances,
68 cestodes themselves are known to excrete or secrete various products that interact with host cells in
69 their vicinity. Cestode larvae-derived factors are known to modulate the activation status of
70 immunocytes such as microglia and dendritic cells (12,13). However, comparatively little is known
71 about how factors contained in, or secreted by, cestode larvae might affect neurons and neuronal
72 networks directly, including whether these may have pro-seizure effects.

73

74 To address this, we used whole-cell patch-clamp recordings and calcium imaging in rodent
75 hippocampal organotypic slice cultures and in acute human cortical brain slices to demonstrate the
76 direct effects of larval products on neuronal activity. We find that both the whole cyst homogenate

and the excretory/secretory (E/S) products of *Taenia crassiceps (T. crassiceps)* and *T. solium* larvae have a strong, acute excitatory effect on neurons. This was sufficient to trigger seizure-like events (SLEs) *in vitro*. Underlying SLE induction was larval induced neuronal depolarization, which was mediated by glutamate receptor activation and not nicotinic acetylcholine receptors, acid-sensing ion channels nor Substance P. Both imaging using glutamate-sensing fluorescent reporters (iGluSnFR) and direct measurements using amino acid assays revealed that the homogenate and E/S products of both *T. crassiceps* and *T. solium* larvae contain high levels of the excitatory amino acid glutamate and to a lesser extent aspartate. Lastly, we provide evidence that larvae of both species, to varying degrees, can produce and release these excitatory amino acids into their immediate environment. This suggests that these parasites release amino acids that could contribute to seizure generation in NCC.

87 *Results*

88 *Taenia crassiceps homogenate excites neurons and can elicit epileptiform activity.*

89 To investigate the potential acute effects of *T. crassiceps* larvae on neurons, *T. crassiceps* larval
90 somatic homogenate was prepared using larvae, harvested from the peritonea of mice, which were
91 freeze-thawed and homogenized (see Materials and Methods and **Fig. 1A**). Whole-cell patch-clamp
92 recordings were made from CA3 pyramidal neurons in rodent hippocampal organotypic brain slice
93 cultures and layer 2/3 pyramidal neurons in human cortical acute brain slices. Pico-litre volumes of *T.*
94 *crassiceps* homogenate were directly applied to the soma of neurons using a custom built pressure
95 ejection system (**Fig. 1A**) (14). Application of the homogenate (20 ms puff) elicited immediate,
96 transient depolarization of the membrane voltage in recordings from rat, mouse and human neurons
97 (**Fig. 1B, C, D**). Increasing the amount of homogenate delivered by increasing the pressure applied to
98 the ejection system resulted in increasingly large membrane depolarization, which could trigger single
99 or multiple action potentials (**Fig. 1B, C, D**). To further explore the acute excitatory effect of
100 *T. crassiceps* on neurons, neuronal networks and the propagation of network activity, we performed
101 fluorescence Ca^{2+} imaging in mouse hippocampal organotypic brain slice cultures. Neurons were
102 virally transfected with the genetically encoded Ca^{2+} reporter, GCAMP6s, under the synapsin promoter
103 and imaged using widefield epifluorescence microscopy (**Fig. 1E** and Materials and Methods). To
104 simulate a pro-ictal environment, a low Mg^{2+} aCSF was used (0.5 mM Mg^{2+}) and neurons in the dentate
105 gyrus were imaged whilst small, spatially restricted puffs of *T. crassiceps* homogenate were delivered
106 every 15 s using a glass pipette (**Fig. 1E**). The cells within the direct vicinity of the puffing pipette
107 showed a sharp increase in fluorescence immediately following the delivery of *T. crassiceps*
108 homogenate (**Fig. 1F t_1**) for all 3 puffs, indicating Ca^{2+} entry following membrane depolarization and
109 action potential generation. Cells in the periphery showed notable increases in fluorescence at a
110 delayed interval following some (but not all) puffs (**Fig. 1F t_2**). The excitation of these cells are likely

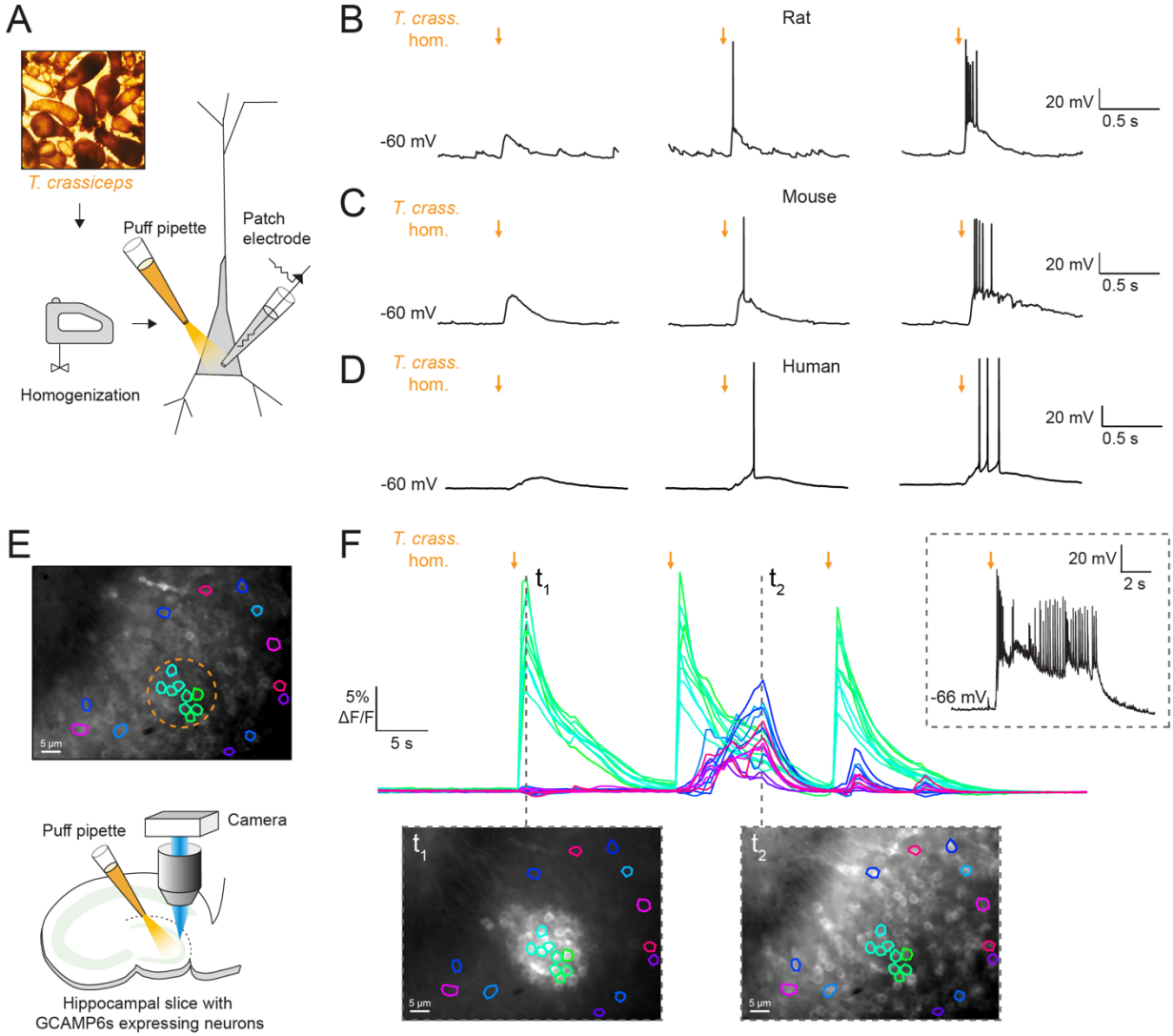

Figure 1: Taenia crassiceps homogenate excites neurons and can elicit epileptiform activity.

A) Schematic showing the experimental set up in which whole-cell patch-clamp recordings were made from CA3 hippocampal pyramidal neurons in rodent organotypic slice cultures while a puff pipette delivered pico-litre volumes of homogenised *Taenia crassiceps* larvae (*T. crass.* hom.) targeted at the cell soma. B) Current-clamp recording from a rat pyramidal neuron while increasing amounts of *T. crass.* hom. was applied via the puff pipette (left to right, orange arrows). Small amounts of *T. crass.* hom. resulted in depolarization (left), increasing amounts elicited single (middle) or even bursts of action potentials (right). C) As in 'B', identical effects of *T. crass.* hom. could be elicited in current-clamp recordings from a CA3 hippocampal pyramidal neuron in a mouse organotypic brain slice culture. D) As in 'B' and 'C', identical effects of *T. crass.* hom. could be elicited in current-clamp recordings from a human frontal lobe layer 2/3 cortical pyramidal neuron in an acute brain slice. E) Top: widefield fluorescence image of neurons in the dentate gyrus of a mouse hippocampal organotypic brain slice culture expressing the genetically encoded Ca^{2+} reporter GCAMP6s under the synapsin promoter in aCSF containing 0.5 mM Mg^{2+}. A subset of neurons used to generate the Ca^{2+} traces in 'E' are indicated by different colours. The orange dotted circle indicates where *T. crass.* hom. was delivered using the puff pipette. Bottom: schematic of the experimental setup including puff pipette and CCD camera for Ca^{2+} imaging using a 470 nm LED. F) Top, dF/F traces representing Ca^{2+} dynamics from the GCAMP6s expressing neurons labelled in 'D' concurrent with 3 puffs (30 ms duration) of *T. crass.* hom. 15 s apart. Bottom: two images of raw Ca^{2+} fluorescence at two time points t_1 and t_2. Note how at time point t_2 neurons distant to the site of *T. crass.* hom. application are also activated, indicating spread of neuronal activity. Inset, top-right: current-clamp recording from a neuron in the region of *T. crass.* hom. application demonstrates seizure-like activity in response to *T. crass.* hom. application.

the result of being synaptically connected to the cells that were exposed to the puff itself. Indeed, a

112 current-clamp recording from a neuron in the same slice (**Fig. 1F, inset**) indicates that a single, spatially
113 restricted puff of *T. crassiceps* homogenate can elicit the onset of a regenerative seizure-like event
114 lasting far longer than the puff itself. Together, these results indicate that *T. crassiceps* larvae
115 homogenate results not just in a transient depolarization of cells in the immediate vicinity of
116 application, but can also trigger a wave of excitation that propagates through the brain slice in both
117 space and time. This demonstrates that *T. crassiceps* homogenate can initiate seizure-like activity
118 under suitable conditions.
119
120 *Tania crassiceps homogenate and E/S product induced neuronal depolarization is mediated by a small*
121 *molecule.*
122 Most cell types tend to have a high $[K^+]_i$, therefore it is conceivable that the *T. crassiceps* homogenate
123 could have a high K^+ concentration, which could potentially account for its depolarizing and excitatory
124 effects on neurons. To address this, we directly measured the ionic composition of the *T. crassiceps*
125 homogenate using a Roche Cobas 6000. The K^+ concentration of the *T. crassiceps* homogenate was
126 11.4 mM as compared to 3.0 mM in our standard aCSF (homogenate $[Na^+]$ was 123.9 mM vs 144.2
127 mM for the aCSF). Direct application of 11.4 mM K^+ via puff pipette during whole-cell current-clamp

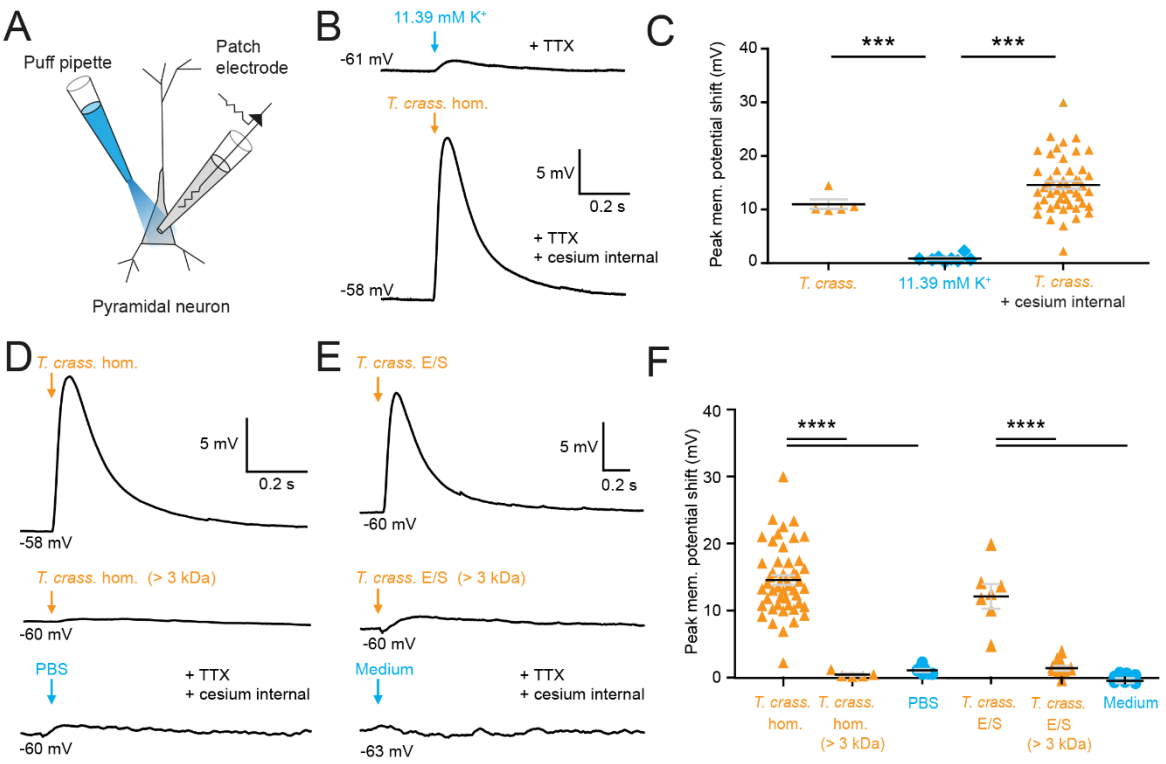

Figure 2: Tania crassiceps homogenate and E/S product induced neuronal depolarization is mediated by a small molecule.

A) Schematic showing the experimental setup in which whole-cell patch-clamp recordings were made from CA3 hippocampal pyramidal neurons in rat organotypic slice cultures while a puff pipette delivered pico-litre volumes targeted at the cell soma. B) Top trace: 20 ms puff of artificial cerebrospinal fluid (aCSF) containing 11.39 mM K^+ (equivalent to the K^+ concentration of *T. crass.* hom.) caused modest depolarization. A standard internal solution was utilised, and 2 µM TTX was added to circulating aCSF to reduce synaptic noise in the voltage trace. Bottom trace: 20 ms puff of *T. crass.* hom. was applied, but a caesium-based internal solution was utilised to block K^+ channels in the presence of TTX. Puffs of *T. crass* hom. resulted in sizeable depolarization. C) Population data showing that responses to 11.39 MM K^+ puffs were significantly smaller than that of the *T. crass.* hom., both when a standard internal solution was utilised (*T. crass.*) and when a caesium internal solution was utilised (*T. crass.* + caesium internal). D) Delivery of *T. crass.* hom. caused a depolarizing shift in membrane potential (top trace). The depolarizing response to *T. crass* hom. was largely abolished by dialysing out all molecules smaller than 3 kDa (middle trace). PBS, the solvent for *T. crass.* hom., did not induce a large neuronal depolarizarion (bottom trace). E) Delivery of a puff of *T. crass.* E/S also caused a depolarizing shift in membrane potential (top trace), which was largely abolished by filtering out all molecules smaller than 3 kDa (middle trace). Culture medium, the solvent for the *T. crass* E/S did not induce depolarization (bottom trace). F) Population data showing that the membrane depolarization induced by the different preparations. Values with mean ± SEM; *** $p \leq 0.001$****, $p \leq 0.0001$.

128 from rat CA3 pyramidal neurons resulted in a modest median positive shift of only 0.72 mV (IQR 0.51

129 - 1.04 mV, N = 8) in the membrane potential, which was significantly less than the depolarization

130 caused by puffs of *T. crassiceps* homogenate (median 10.12 mV, IQR 9.93 - 12.49 mV, N = 5, p = 0.0016,

131 Mann-Whitney U test, **Fig. 2A, B, C**). Puffs of aCSF containing 11.4 mM K^+ were directed toward the

132 soma of recorded neurons. Whilst this did cause a depolarization of the membrane potential, the

133 effect was modest, a median positive shift of only 0.72 mV (IQR 0.51 - 1.04 mV, N = 8) in the membrane

134 potential, which was significantly less than the depolarization caused by puffs of *T. crassiceps*
135 homogenate (median 10.12 mV, IQR 9.93 - 12.49 mV, N = 5, p = 0.0016, Mann-Whitney U test, **Fig. 2B,**
136 **C**). Next, to isolate neuronal depolarization induced by *T. crassiceps* homogenate, but not mediated
137 by K^+, a caesium based internal solution was used. The addition of caesium did not greatly change the
138 positive shift in membrane potential caused by *T. crassiceps* homogenate (median 13.76, IQR 10.87 -
139 17.24 mV, N = 49, p ≤ 0.0489, Mann-Whitney U test, **Fig. 2C, D**). Together, this indicates that although
140 K^+ in the *T. crassiceps* homogenate does contribute to membrane depolarization, the majority of the
141 effect is mediated by a different component.
142
143 To determine the fraction of the *T. crassiceps* homogenate, which underlies the acute excitatory effect
144 on neurons we observed, we used a dialysis membrane to separate the fraction of the homogenate
145 bigger than 3 kDa from the total homogenate. This removed molecules smaller than 3 kDa from the
146 homogenate. When this dialysed *T. crassiceps* was puffed onto the cells in the same recording
147 conditions as in **Fig. 2B**, the depolarizing response was greatly reduced (p ≤ 0.0003, Mann-Whitney U
148 test, **Fig. 2D, F**). The median positive shift in membrane potential for dialysed *T. crassiceps*
149 homogenate was only 0.27 mV (IQR 0.20 - 0.85 mV, N = 5) as compared to a median of 13.76 mV (IQR
150 10.87 - 17.24 mV, N = 49) for the total homogenate. Phosphate buffered saline, the solvent for the
151 homogenate also did not produce substantial depolarisation (**Fig. D, F**). This suggests that the
152 excitatory component of the *T. crassiceps* homogenate is a molecule smaller than 3 kDa.
153
154 Given that helminths are well known to excrete or secrete (E/S) products into their immediate
155 environment, we next sought to determine whether the <3kDa small molecule/s from *T. crassiceps*
156 homogenate, which was found to induce in neuronal depolarisation, was also produced as an E/S
157 product generated by *T. crassiceps* larvae. The media was collected over a period of 21 days and either
158 used unaltered (*T. crassiceps* total E/S products) or buffer exchanged into a > 3 kDa fraction using an
159 Amicon stirred cell. Brief application of total *T. crassiceps* E/S products using a soma directed puff was

160 sufficient to cause neuronal depolarization (mean 12.29 mV, SEM 1.74 mV, N = 7) significantly larger
161 than that of the media control (mean -0.48 mV, SEM 0.40 mV, N = 7, $p \leq 0.001$, One-way ANOVA,
162 Tukey's post hoc test, **Fig. 2E, F**). However, the *T. crassiceps* E/S product fraction larger than 3 kDa
163 (mean 1.43 mV, SEM 0.43 mV, N = 8) did not generate significant neuronal depolarization as compared
164 to control (mean 1.10 mV, SEM 0.22 mV, N = 8, **Fig. 2E, F**). Together this set of experiments
165 demonstrated that both *T. crassiceps* homogenate and *T. crassiceps* E/S products contain an
166 excitatory component, which is a small molecule.
167
168 *The excitatory effects of Taenia crassiceps are mediated by glutamate receptor activation.*
169 Robinson *et al* (2012) have found Substance P, an abundant neuropeptide and neurotransmitter, in
170 close vicinity to human NCC granulomas (11). We therefore investigated whether Substance P could
171 elicit a similar neuronal depolarizing response to that of *T. crassiceps* homogenate. However, we
172 found that 100 µM Substance P had no acute effect on the membrane potential of CA3 hippocampal
173 pyramidal neurons (median = 0.08 mV, IQR 0.01 – 0.12 mV, N = 5, Wilcoxon signed rank test with
174 theoretical median = 0.00, p = 0.0625, **Fig. 3A, B**).

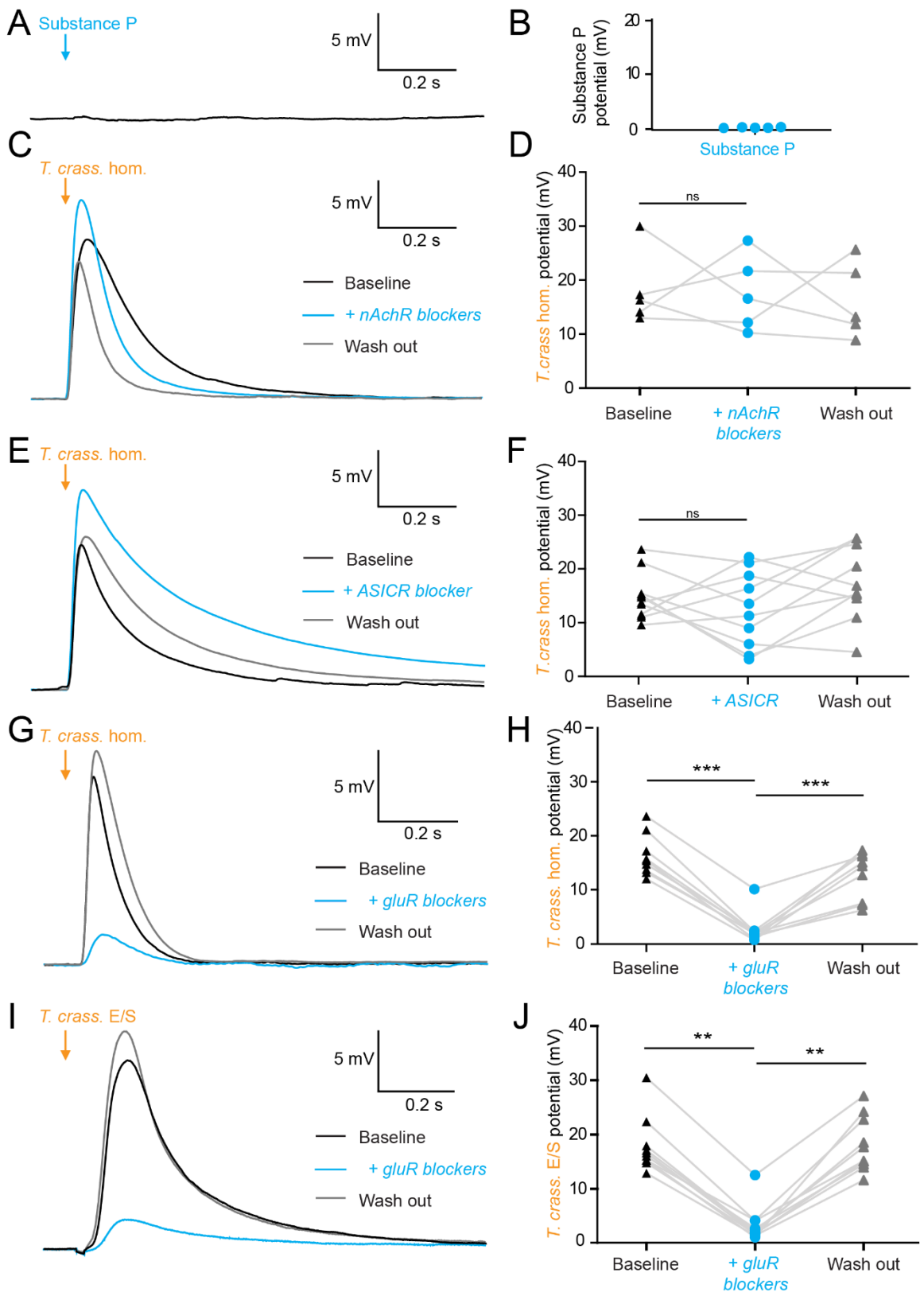
A
Substance P
5 mV
0.2 s
B
Substance P potential (mV)
20
10
0
Substance P
C
T. crass. hom.
5 mV
0.2 s
Baseline
+ nAchR blockers
Wash out
D
T.crass hom. potential (mV)
40
30
20
10
0
ns
Baseline
+ nAchR blockers
Wash out
E
T. crass. hom.
5 mV
0.2 s
Baseline
+ ASICR blocker
Wash out
F
T.crass hom. potential (mV)
40
30
20
10
0
ns
Baseline
+ ASICR
Wash out
G
T. crass. hom.
5 mV
0.2 s
Baseline
+ gluR blockers
Wash out
H
T. crass. hom. potential (mV)
40
30
20
10
0
***
***
Baseline
+ gluR blockers
Wash out
I
T. crass. E/S
5 mV
0.2 s
Baseline
+ gluR blockers
Wash out
J
T. crass. E/S potential (mV)
40
30
20
10
0
**
**
Baseline
+ gluR blockers
Wash out

175

176

Figure 3: The excitatory effects of Taenia crassiceps are mediated by glutamate receptor activation.
Whole-cell patch-clamp recordings in current-clamp were made from CA3 pyramidal neurons in rat organotypic hippocampal slices using a cesium-based internal in the presence of 2 µM TTX. A) 20 ms puff of Substance P (100 µM) via a puff pipette directed at the soma did not affect neuronal membrane potential. B) Population data for Substance P application. C) The depolarizing response to a *T. crass.* hom. puff before (black trace), in the presence of (blue trace), and following wash out of (grey trace), a nicotinic acetylcholine receptor (nAchR) blocker (mecamylamine hydrochloride, 10 µM). D) Population data demonstrating that nAchR blockade has no significant effect on *T. crass.* hom. induced depolarization. E) Depolarizing response to a *T. crass* hom. puff before (black trace), in the presence of (blue trace), and following washout of (grey trace), an ASIC receptor blocker (amiloride, 2 mM) F) Population data demonstrating that ASIC receptor blockade has no significant effect on *T. crass.* hom. induced depolarization. G) Depolarizing response to a *T. crass.* hom. puff before (black trace), in the presence of (blue trace), and following washout of (grey trace), a pharmacological cocktail to block glutamate receptors (10µM CNQX, 50µM D-AP5 and 2 mM kynurenic acid). ***$p \leq 0.001$ H) Population data showing that the depolarization response to *T. crass.* hom. is significantly reduced in the presence of glutamate receptor blockers and returns upon wash out. I) Depolarizing response to a puff of *T. crass* excretory/secretory (E/S) products is also markedly reduced during glutamate receptor blockade. J) Population data showing that the depolarization response to *T. crass.* hom. is significantly reduced in the presence of glutamate receptor blockers and returns upon wash out. ***$p \leq 0.01$, **$p \leq 0.01$.

Next we tested whether nicotinic acetylcholine receptors (nAchRs), well described ionotropic receptors in the nervous system (15), could elicit neuronal depolarisation. However we found that blockade of nAchRs with mecamylamine hydrochloride (10µM) did not significantly alter the *T. crassiceps* homogenate induced depolarisation. The median *T. crassiceps* homogenate induced depolarization was 16.28 mV (IQR 13.54 - 23.63 mV) during baseline, 16.58 mV (IQR 11.21 - 24.50 mV) in the presence of mecamylamine hydrochloride and 13.20 mV (IQR = 10.37 - 23.48 mV) following washout (N = 5, p = 0.6914, Friedman test, **Fig. 3C, D**). Acid-sensing ion channels (ASICs) are proton-gated sodium channels known to be expressed by hippocampal neurons and result in neuronal depolarization when activated. However, blockade of ASICs with the non-specific ASIC blocker amiloride (2 mM) did not significantly attenuate the effect of the homogenate (**Fig. 3C**), with the mean *T. crassiceps* homogenate induced depolarization being 14.55 mV (SEM 1.41 mV) during baseline, 12.12 mV (SEM 2.25 mV) in the presence of amiloride, and 17.06 mV (SEM 2.20 mV) following washout (N = 10, p = 0.1124, repeated measures ANOVA, **Fig. 3C, D**).

Ionotropic glutamate receptors (GluRs) including α-amino-3-hydroxy-5-methyl-4-isoxazoleproprionic acid (AMPA), Kainate and N-methyl-D-aspartate (NMDA) receptors (16) are the major source of fast neuronal depolarisation in neurons, therefore it is likely that *T. crassiceps* homogenate could cause

195 neuronal depolarization by activation of GluRs. To test this possibility, *T. crassiceps* homogenate-
196 induced neuronal depolarization was measured before, during and after the application of 10µM
197 CNQX, 50µM D-AP5 and 2mM kynurenic acid (in the aCSF) to block all three classes of GluRs (all in the
198 presence of TTX and using a caesium internal solution). We found that GluR blockade significantly
199 reduced the median *T. crassiceps* homogenate induced neuronal depolarization from 14.72 mV (IQR
200 13.39 - 15.68 mV) to 1.90 mV (IQR 1.09 - 2.21 mV, N = 9, $p \leq 0.01$, Friedman test with Dunn's multiple
201 comparison test, **Fig. 3G, H**), which recovered to a median value of 14.37 mV (IQR 7.32 - 16.38 mV)
202 following washout (N = 9, $p \leq 0.01$, Friedman test with Dunn's multiple comparison test, **Fig. 3G, H**).
203 Similarly for *T. crassiceps* E/S products we found that application of GluR antagonists reduced the
204 median total *T. crassiceps* E/S products induced depolarization from 16.35 mV (IQR 15.17 - 19.03 mV)
205 to 2.19 mV (IQR 1.67 - 4.16 mV, N = 10, $p \leq 0.01$, Friedman test with Dunn's multiple comparison test,
206 **Fig. 3I, J**), which recovered to a median value of 16.43 mV (IQR 14.41 - 23.14 mV) following washout
207 (N = 10, $p \leq 0.01$, Friedman test with Dunn's multiple comparison test, **Fig. 3I, J**). These results indicate
208 that the acute excitatory effect of both *T. crassiceps* homogenate and *T. crassiceps* E/S products is
209 mediated through GluRs.
210
211 *Taenia crassiceps products contain excitatory amino acids detected using iGluSnFR*
212 Glutamate is the prototypical agonist of GluRs (16). We therefore sought to directly detect glutamate
213 in *T. crassiceps* larval products using glutamate-sensing fluorescent reporters. We utilized the
214 genetically encoded glutamate reporter (iGluSnFR), which was virally transfected into mouse
215 organotypic hippocampal slice cultures under the synapsin 1 gene promoter and imaged using
216 widefield epifluorescence microscopy (**Fig. 4A** and Materials and Methods). Brief puffs of *T. crassiceps*
217 homogenate delivered over the soma of iGluSnFR-expressing neurons generated robust increases in
218 fluorescence (**Fig. 4B**). Similar fluorescence increases were observed with puffs of *T. crassiceps* E/S
219 products (**Fig. 4C**). Aspartate has a similar chemical structure to glutamate and is also known to excite
220 neurons via glutamate receptor activation (17). iGluSnFR is also known to be sensitive to aspartate as

221 well as glutamate (18). We found that puffing aCSF containing 100 µM glutamate or 100 µM aspartate

222 onto hippocampal pyramidal neurons expressing iGluSnFR resulted in similarly sized fluorescence

223 transients (**Fig. 4D-G**). Similarly, puffing aCSF containing 100 µM glutamate or 100 µM aspartate during

224 whole-cell current-clamp recordings both elicited membrane depolarizations which were similar those

225 observed with *T. crassiceps* homogenate and E/S products (**Fig. 4H, I**).

226

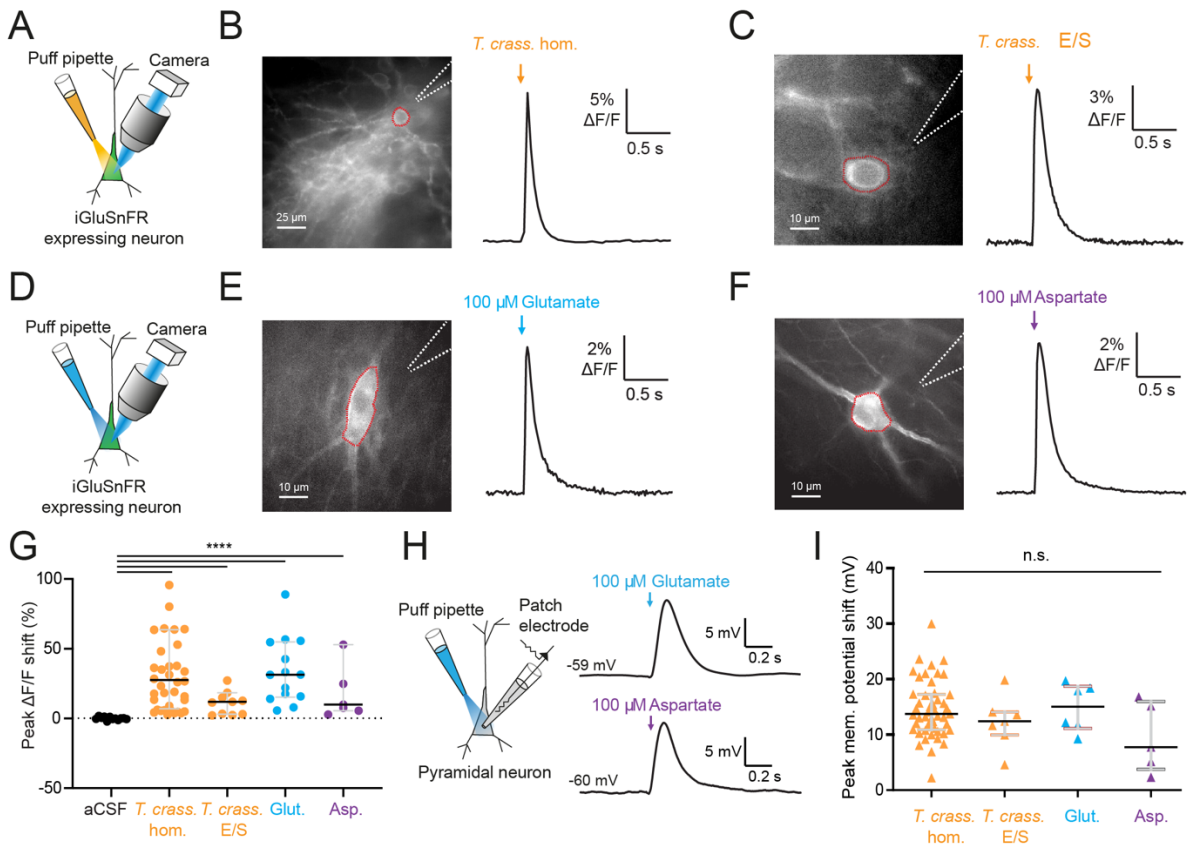

Figure 4: Taenia crassiceps products contain excitatory amino acids detected using iGluSnFR.
A) Schematic of the experimental setup for glutamate detection by the genetically encoded fluorescent glutamate reporter iGluSnFR, including puff pipette and sCMOS camera for imaging following excitation using a 475/28 nm LED-based light engine. B) Left, iGluSnFR expressing neuron with the region of interest (red dashed line) used to calculate dF/F trace (right) during a 20 ms *T. crassiceps* homogenate (*T. crass.* hom.) puff (orange arrow). C) As in 'B' but with a 20 ms *T. crassiceps* excretory/secretory product (*T. crass.* E/S) puff (orange arrow). D) Schematic of experimental setup as in 'A' but with glutamate or aspartate application via puff pipette. E) iGluSnFR fluorescence just after a 20 ms puff of aCSF containing 100 µM glutamate. F) As in 'E' but with iGluSnFR fluorescence during a 20 ms puff of aCSF containing 100 µM aspartate (purple arrow). G) Population data comparing peak dF/F shifts after a 20 ms puff of aCSF (as a negative control), *T. crass.* hom., *T. crass.* E/S, aCSF containing 100 µM glutamate, or aCSF containing 100 µM aspartate (values with medians ± IQR;). H) Schematic of whole-cell patch-clamp recording in current-clamp mode from a CA3 pyramidal neuron using a cesium-based internal and in the presence of 2 µM TTX. 20 ms puff of aCSF containing 100 µM glutamate produces a significant depolarizing shift in membrane potential (top trace), a similar puff but with 100 µM aspartate elicited a similar response (bottom trace). I) Population data comparing peak membrane potential shift after a 20 ms puff of *T. crass.* hom., *T. crass.* E/S, aCSF containing 100 µM glutamate, or aCSF containing 100 µM aspartate. Values with medians ± IQR; ns = not significant, **** $p \leq 0.0001$.

227 *Taenia crassiceps larvae contain and produce glutamate and aspartate*

228 Given the short-term responses to homogenate and E/S products we observed using iGluSnFR, we
229 next sought to record possible evidence of changes in ambient glutamate or aspartate using a more
230 naturalistic setting where iGluSnFR-expressing neurons were placed adjacent to a live *T. crassiceps*
231 larvae (see Materials and Methods, **Fig. 5A-C**). During imaging periods lasting up to 15 minutes,
232 fluorescence was stable, indicating no detectable oscillatory changes in ambient glutamate/aspartate
233 on the timescales recorded (N = 5, **Fig. 5B, C**). We then directly measured the concentration of
234 glutamate and aspartate in our *T. crassiceps* products using separate glutamate and aspartate assays
235 (see Materials and Methods). We found that the mean concentration of glutamate in the *T. crassiceps*
236 homogenate and E/S products was 114.6 µM (SEM 18.0 µM, N = 5, **Fig. 5D**) and 119.5 µM (SEM 13.3
237 µM, N = 6, **Fig. 5D**) respectively. The concentration of aspartate in *T. crassiceps* homogenate and E/S
238 products was 25.8 µM (SEM 5.4 µM, N = 3, **Fig. 5E**) and 48.7 µM (SEM 19.5 µM, N = 3, **Fig. 5E**)
239 respectively. Together, these findings suggest that *T. crassiceps* larval homogenate and E/S products
240 contain the excitatory amino acids glutamate and aspartate at concentrations that are sufficient to
241 elicit neuronal depolarization.

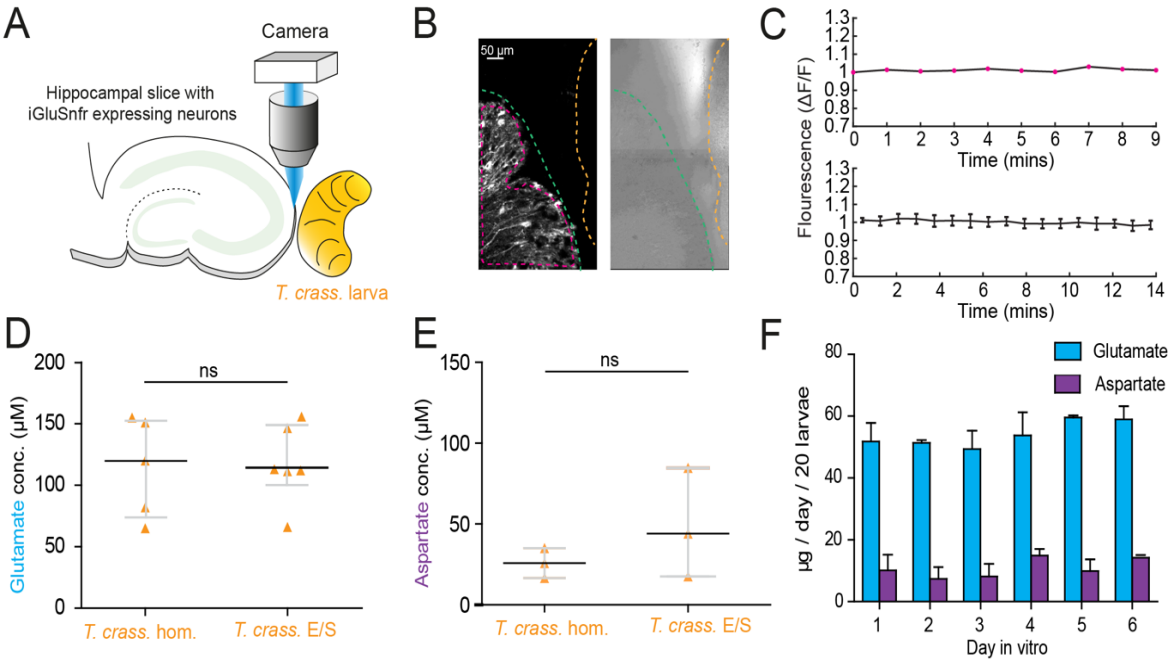

Figure 5: Taenia crassiceps larvae contain and produce glutamate and aspartate.

A) Schematic of the experimental setup whereby a living *Taenia crassiceps* (*T. crass.)* larva is placed in close proximity to a hippocampal organotypic brain slice with iGluSnFR-expressing neurons for detection of glutamate fluctuations. B) Left, fluorescence image of a slice with iGluSnFR-expressing neurons (green dashed line) adjacent to a *T. crass.* larva (orange dashed line), also visible in the transmitted light image (right). The region of interest (pink dashed line) was used to calculate the top dF/F trace in 'C'. C) Top, dF/F trace from the example in 'B' during a 9 minute recording. Lower trace: population data of the mean ± SEM from 5 slice-larva pairs showed no detectable oscillations or changes in glutamate. D) Glutamate concentration in *T. crass.* Homogenate (*T. crass.* hom.) and *T. crass.* excretory/secretory products (*T. crass*. E/S) as measured using a glutamate assay kit. E) Aspartate concentration in *T. crass.* hom. and *T. crass.* E/S as measured using an aspartate assay kit. Values with medians ± IQR; ns = not significant, $p > 0.05$ F). *De novo* production of glutamate and aspartate by *T. crass.* larvae over a 6-day culture period (means ± SEM, N = 3).

Next, to determine whether *T. crassiceps* larvae actively produce and excrete/secrete glutamate and/or aspartate into their environments we measured the *de novo* daily production of glutamate and aspartate by larvae following harvest of live larvae. *T. crassiceps* larvae released a relatively constant mean daily amount of both glutamate (day 1: 51.8 µg/20 larvae, SEM 6.0 µg/20 larvae, N = 3; day 2: 51.4 µg/20 larvae, SEM 0.9 µg/20 larvae. N = 3; day 3: 49.4 µg/20 larvae, SEM 5.9 µg/20 larvae, N = 3; day 4: 53.8 µg/20 larvae, SEM 7.4, N = 3; day 5: 59.6 µg/20 larvae, SEM 0.7, N = 3; day 6: 59.0 µg/20 larvae, SEM = 4.3, N = 3, Fig. 5F) and aspartate (day 1: 10.1 µg/20 larvae, SEM 5.1 µg/20 larvae, N = 3; day 2: 7.4 µg/20 larvae, SEM 3.8 µg/20 larvae. N = 3; day 3: 8.2 µg/20 larvae, SEM 4.1 µg/20 larvae, N = 3; day 4: 14.9 µg/20 larvae, SEM 2.2, N = 3; day 5: 9.9 µg/20 larvae, SEM 3.8, N = 3; day 6: 14.2 µg/20 larvae, SEM = 0.9, N = 3, **Fig. 5F**) per day.

253

254 *Taenia solium larvae depolarize human neurons via the production of glutamate*

255 *T. crassiceps*, whilst a closely related species to *T. solium*, is not the causative pathogen in humans.
256 We therefore sought to determine whether homogenate and E/S products from *T. solium* (the natural
257 pathogen in humans), also have an excitatory effect on human neurons within human brain tissue (the
258 natural host). During whole-cell patch-clamp recordings made from human layer 2/3 pyramidal cells
259 in acute cortical brain slices, pico-litre volumes of *T. solium* larval homogenate and *T. solium* larval E/S
260 products were delivered by a glass pipette. Similarly, to the case with *T. crassiceps*, both *T. solium*
261 homogenate (**Fig. 6A**) and *T. solium* E/S product (**Fig. 6A**) caused membrane depolarization, which was
262 sufficient to result in action potential firing.

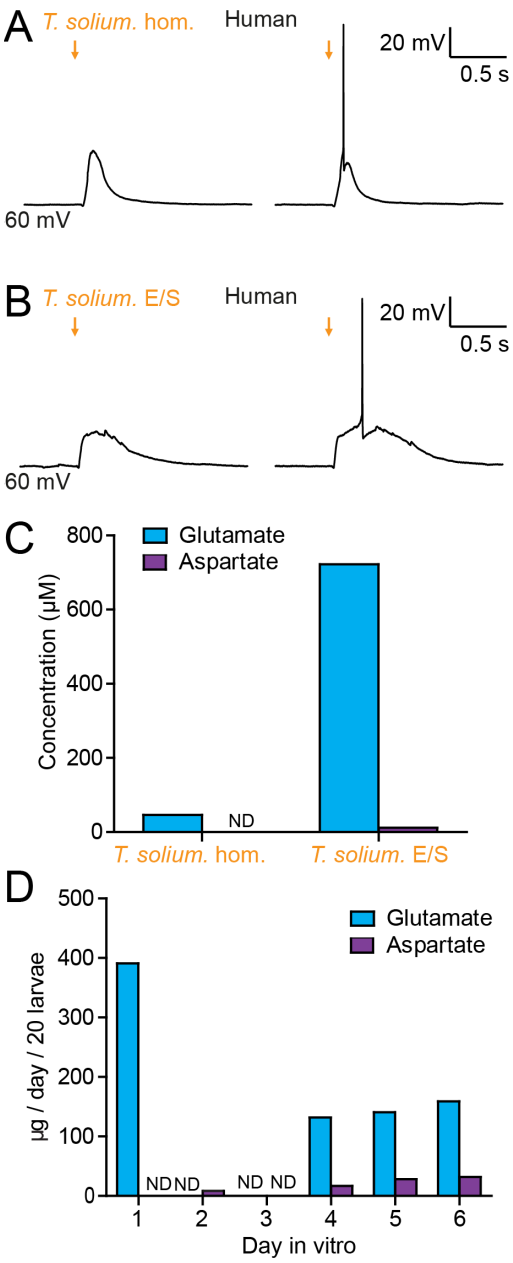

Figure 6: Taenia solium larvae depolarize human neurons via the production of glutamate.
A) Whole-cell patch-clamp recordings in current-clamp from a layer 2/3 human frontal lobe cortical pyramidal neuron in an acute brain slice, while increasing amounts of *T. solium* homogenate (*T. solium* hom.) was applied via a puff pipette (left to right, orange arrows). Small amounts of *T. solium* hom. resulted in depolarization (left), while an increased amount elicited an action potential (right). B) As in 'A', *T. solium* excretory/secretory products (*T. solium* E/S) elicited membrane depolarization and an increased amount elicited an action potential. C) Concentrations of glutamate and aspartate in *T. solium* hom. and *T. solium* E/S (N = 1, ND = not detectable). D) *De novo* production of glutamate and aspartate by *T. solium* larvae over a 6-day culture period (N = 1, ND = not detectable).

We then measured the glutamate and aspartate concentration of the *T. solium* homogenate and *T. solium* E/S products. Significant levels of glutamate were detected in both *T. solium* homogenate (46.4 µM, N = 1, **Fig. 6C**) and the *T. solium* E/S product (722 µM, N=, **Fig. 6C**). However, aspartate was undetectable in the *T. solium* homogenate (N = 1, **Fig. 6C**) with a low concentration of aspartate observed in the E/S product (15.3 µM, N = 1, **Fig. 6C**). Finally, *T. solium* larvae were observed to release glutamate on the first day post-harvest (391.1 µM/20 larvae, N = 1, **Fig. 6D**) none on the 2nd and 3rd day *in vitro* (N = 1, **Fig. 6D)**, but produced significant amounts of glutamate on days 4, 5 and 6 (day 4: 131.9 µM/20 larvae, N = 1; day 5: 140.6 µM/20 larvae, N = 1; day 6: 158.8 µM/20 larvae, N = 1, **Fig. 6D**). Aspartate was not detected on days 1 and 3 (N = 1, **Fig. 6D**), but was observed to be released on days 2, 4, 5 and 6 (day 2: 8.4 µM/20 larvae, N = 1; day 4: 16.8 µM/20 larvae, N = 1; day 5: 28.1 µM/20 larvae N = 1; day 6: 31.9 µM/20 larvae, N = 1, **Fig. 6D**). These results demonstrate that *T. solium* larvae continually release glutamate and aspartate (albeit to different degrees) into their immediate surroundings.

281 *Discussion*

282 Here we used patch-clamp electrophysiology, and calcium imaging in rodent hippocampal organotypic
283 slice cultures and human acute cortical slices to demonstrate that cestode larval products cause
284 neuronal depolarization and can initiate seizure-like events via glutamate receptor activation.
285 Glutamate-sensing fluorescent reporters and amino acid assays revealed that *T. crassiceps* and
286 *T. solium* larvae contain and release the excitatory amino acid glutamate and to a lesser extent
287 aspartate.

288

289 Clinical evidence and animal models conclusively demonstrate that the presence of cestode larvae in
290 the brain can result in the generation of seizures (10,19). Previous work has focused on the
291 involvement of the host inflammatory response in seizure generation (11,20). Whilst this is likely
292 important, it does not preclude the involvement of additional or exacerbating pathogenic mechanisms
293 for seizure generation and epileptogenesis in NCC. In this study we have identified that *Taenia* larvae
294 have a direct excitatory effect on neurons via glutamatergic signaling. This is important, as the central
295 role of glutamatergic signaling in epileptogenesis has conclusively been shown using multiple cell
296 culture (21–23), slice (24–26), and *in vivo* models of epilepsy (27–29).

297

298 Clinically, in addition to NCC, the other major causes of adult acquired epilepsy are stroke, traumatic
299 brain injury and CNS tumors (30,31). In these other causes of acquired epilepsy, glutamatergic
300 signaling and glutamate excitotoxicity are thought to be central to the pathogenic process. Glutamate
301 excitotoxicity occurs when depolarized, damaged or dying neurons release glutamate, which activate
302 surrounding neurons via NMDA and AMPA receptors, resulting in sustained neuronal depolarization,
303 Ca^{2+} influx and the subsequent activation of signaling cascades and enzymes. These in turn lead to cell
304 death via necrosis and apoptosis (32), the further release of intracellular glutamate and the
305 propagation of the excitotoxic process to neighbouring cells. In the neurons that survive, the
306 prolonged exposure to glutamate has been shown to cause hyperexcitability and seizures (21,23) via

307 multiple mechanisms including enhanced intrinsic excitability and NMDA receptor dependent
308 disruption of GABAergic inhibition (33–35). Given our finding that cestode larvae contain and release
309 significant quantities of glutamate, it is possible that should homeostatic mechanisms for taking up
310 and metabolizing glutamate fail to compensate for larval-derived glutamate in the extracellular space,
311 similar glutamate-dependent excitotoxic and epileptogenic processes that occur in stroke, traumatic
312 brain injury and CNS tumors are likely to also occur in NCC.
313
314 Glioma, a common adult primary brain tumor, which typically presents with seizures in over 80% of
315 patients (36), is an intriguing condition for comparison to NCC. Here, the tumor cells themselves have
316 been shown to release glutamate into the extracellular space via the system x_c^-cystine-glutamate
317 antiporter (35). Interestingly, there is compelling evidence that tumoral release of glutamate via this
318 mechanism both causes seizures and favours glioma preservation, progression and invasion in cases
319 of malignant glioma (37–39). Analogously it is possible that *Taenia* larvae in the brain utilize the
320 release of glutamate and the induction of glutamate excitotoxicity to facilitate their growth and
321 expansion, with the accompanying effect of seizure generation. In addition, the death of *Taenia* larvae,
322 or larval-derived cells, would also result in the release of metabolic glutamate, further contributing to
323 glutamate release and excitotoxicity. In the case of glioma, where the mechanism of glutamate release
324 by tumor cells is known, pharmacological agents (*e.g.,* sulfasalazine), which block glutamate release
325 have considerable potential as therapeutic agents for reducing seizure burden in this condition.
326 Therefore, it is important that future work attempts to identify the molecular mechanisms underlying
327 the *Taenia*-specific production of glutamate to inform the development of new therapeutic strategies
328 to potentially reduce larval expansion and possibly treat seizures in NCC.
329
330 An important consideration is how we might reconcile our findings of glutamate release by *Taenia*
331 larvae with the clinical picture of delayed symptom onset in NCC. In people with NCC, some experience
332 acute seizures immediately following infection whilst others present with seizures months to years

333 following initial infection (40,41). This suggests that multiple different, or possibly interacting,
334 mechanisms might be involved in the epileptogenic process in NCC. A recent report has shown that *T.*
335 *solium* cyst products mimicking viable cysts contain the enzyme glutamate dehydrogenase, which
336 metabolizes glutamate, whilst products mimicking degenerating cysts do not (42). This predicts that
337 the glutamate levels the brain would be exposed to would be highest when a cyst dies and releases
338 its contents into its immediate surroundings. Neuroinflammation has long been thought to be central
339 to the development of seizures in NCC. In support of this, larval suppression of host inflammatory
340 responses could help explain why many patients may remain asymptomatic for years following
341 infection. Our findings are not at odds with this line of thinking when considering the effect of
342 neuroinflammation on extracellular glutamate uptake. In the healthy brain parenchymal astrocytes
343 are optimized to maintain extracellular glutamate at low concentrations (43). However, the
344 inflammatory transition of astrocytes to a reactive phenotype is known to impede their ability to
345 buffer uptake of extracellular glutamate (44). It is therefore conceivable that cyst-associated reactive
346 astrocytosis may gradually erode the ability of homeostatic mechanisms to compensate for larvae
347 derived extracellular glutamate resulting in delayed symptom onset in NCC.
348
349 There is still considerable uncertainty regarding the precise sequence of events leading to seizure
350 onset in NCC. Nonetheless our findings provide the first evidence that, as is the case with the other
351 common causes of adult-acquired epilepsy (*i.e.* stoke, traumatic brain injury and glioma), increased
352 extracellular, parasite-derived excitatory amino acids such as glutamate, and perturbed glutamatergic
353 signaling, possibly also play a role in the development of seizures in NCC.
354
355
356
357
358

359 *Materials and Methods*

360 *Ethics statement*

361 All animal handling, care and procedures were carried out in accordance with South African national
362 guidelines (South African National Standard: The care and use of animals for scientific purposes, 2008)
363 and with authorisation from the University of Cape Town Animal Ethics Committee (Protocol No: AEC
364 015/015, AEC 014/035). Ethical approval for use of human tissue was granted by the University of
365 Cape Town Human Research Ethics Committee (HREC 016/2018) according to institutional guidelines.

366

367 *Taenia maintenance and preparation of whole cyst homogenates and E/S products*

368 Larvae of *T. crassiceps* (ORF strain) were donated to us by Dr Siddhartha Mahanty (University of
369 Melbourne, Melbourne, Australia) and propagated *in vivo* by serial intraperitoneal infection of 5–8-
370 week-old female C57BL/6 mice. Every 3 months parasites were harvested by peritoneal lavage and
371 washed once in phosphate buffered saline (PBS, 1X, pH 7.4) containing penicillin (500 U/ml);
372 streptomycin (500 ug/ml); and gentamicin sulphate (1000 ug/ml) (Sigma-Aldrich), before being
373 washed a further five times in standard PBS (1X).

374

375 For the preparation of *T. crassiceps* whole cyst homogenate, larvae were stored immediately after
376 harvesting at -80 °C. Later the larvae were thawed (thereby lysing the cells) and suspended in PBS (1X)
377 containing a protease cocktail inhibitor (1% vol/vol, Sigma-Aldrich) at a larval:PBS ratio of 1:3. The
378 larvae were then homogenised on ice using a Polytron homogenizer (Kinematica). The resulting
379 mixture was centrifuged at 4000rpm for 20 minutes at 4 °C. The liquid supernatant (between the white
380 floating layer and solid pellet) was collected and sterile filtered through a 0.22 µm size filter (Millex-
381 GV syringe filter, Merck). This supernatant was then aliquoted and stored at -80 °C until use. To assess
382 whether large or small molecules were responsible for the excitation of neurons, a portion of the
383 whole cyst homogenate was dialysed using a Slide-A-Lyzer™ dialysis cassette (3kDa MWCO,
384 Separations) in 2l of artificial cerebro-spinal fluid (aCSF) at 4 °C. The aCSF solution was changed twice

385 over 24 hours. To determine the ionic composition of *T. crassiceps* whole cyst homogenate a Cobas
386 6000 analyser (Roche) was used, with ion specific electrodes for K^+ and Na^+. A Mettler Toledo
387 SevenCompact™ pH meter S210 (Merck) was used to determine the pH of the homogenate.
388 For the preparation of *T. crassiceps* excretory/secretory products, after harvesting, washed larvae
389 were maintained for 14-21 days at 37 °C in 5 % CO_2 in 50 ml tissue culture flasks (approximately 7 ml
390 volume of larvae per flask) containing culture medium consisting of Earle's Balanced Salt Solution
391 (EBSS) supplemented with glucose (5.3 g/liter), Glutamax (1X), penicillin (50 U/ml), streptomycin
392 (50 ug/ml), gentamicin sulphate (100 ug/ml) and nystatin (11.4 U/ml) (Sigma-Aldrich). Culture
393 medium was replaced after 24 hours, and the original media discarded. Thereafter, culture media
394 were replaced and collected every 48-72 hours, stored at -20 °C and at the end of the culture period,
395 thawed and pooled. The pooled conditioned medium was termed total excretory/secretory products
396 (total E/S). A portion of the total E/S was aliquoted and stored at -80 °C, while another portion was
397 concentrated (about 100X) and buffer exchanged to PBS using an Amicon stirred cell with a 3 kDa
398 MWCO cellulose membrane (Sigma-Aldrich). The concentrated product contained *T. crassiceps* E/S
399 products larger in size than 3kDa (E/S > 3kDa), in PBS (1X). This was aliquoted and stored at -80 °C.
400 The fraction of the total E/S that passed through the 3kDa membrane (E/S < 3 KDa, still in medium)
401 was also retained, aliquoted and stored at -80 °C.
402 For the preparation of *T. solium* whole cyst homogenate, larvae of *T. solium* were harvested from the
403 muscles of a heavily infected, freshly slaughtered pig. After extensive washing with sterile 1X PBS,
404 *T. solium* larvae were suspended in PBS containing phenylmethyl-sulphonyl fluoride (5mM) and
405 leupeptin (2.5 µM) at a larvae:PBS ratio of 1:3. Larvae were then homogenised using a sterile handheld
406 homogenizer at 4 °C. The resulting homogenate was sonicated (4 x 60 s at 20 kHz, 1 mA, with 30 s
407 intervals) and gently stirred with a magnetic stirrer for 2 h at 4 °C. Thereafter it was centrifuged at
408 15,000 g for 60 min at 4 °C and the liquid supernatant (between the white floating layer and solid
409 pellet) was collected. The supernatant was filtered through 0.45 µm size filters (Millex-GV syringe

410 filter, Merck), aliquoted and stored at -80 °C. All *T. crassiceps* and *T. solium* larval products were
411 assessed for protein concentration using a BCA protein or Bradford's assay kit respectively.

412 For the assessment of daily glutamate and aspartate production both *T. crassiceps and*
413 *T. solium* larvae were placed into 6 well plates (+/- 20 per well, of roughly 5mm length) with 2 ml of
414 culture medium (*Taenia solium* medium: RPMI 1640 with 10 mM HEPES buffer, 100 U/ml penicillin,
415 100 µg/ml streptomycin, 0.25 µg/ml amphotericin B and 2 mM L-glutamine; *Taenia*
416 *crassiceps* medium: EBSS with 100 U/ml penicillin, 100 µg/ml streptomycin, 11.4 U/ml nystatin and 2
417 mM Glutamax). Every 24 hours 1 ml of culture medium was collected from each well, stored at -80 °C,
418 and replaced with fresh culture medium. The concentrations of glutamate and aspartate were
419 measured using a Glutamate assay kit and an Aspartate assay kit, respectively, according to the
420 supplier's instructions (Sigma-Aldrich). "*T. solium* E/S" used in human organotypic brain slice
421 electrophysiology experiments, consisted of a mixture of equal volumes of the *T. solium* medium
422 collected on D1, D2 and D3.

423

424 *Brain slice preparation*

425 Rodent hippocampal organotypic brain slices were prepared using 6-8 day old Wistar rats and C57BL/6
426 mice following the protocol originally described by Stoppini et al., (1991). Brains were extracted and
427 swiftly placed in cooled (4 °C) dissection media consisting of Earle's balanced salt solution (Sigma-
428 Aldrich); 6.1 g/L HEPES (Sigma-Aldrich); 6.6 g/L D-glucose (Sigma-Aldrich); and 5 µM sodium hydroxide
429 (Sigma-Aldrich). The hemispheres were separated, and individual hippocampi were removed and
430 immediately cut into 350 µm slices using a McIlwain tissue chopper (Mickle). Cold dissection media
431 was used to rinse the slices before placing them onto Millicell-CM membranes (Sigma-Aldrich). Slices
432 were maintained in culture medium consisting of 25 % (vol/vol) Earle's balanced salt solution (Sigma-
433 Aldrich); 49 % (vol/vol) minimum essential medium (Sigma-Aldrich); 25 % (vol/vol) heat-inactivated
434 horse serum (Sigma-Aldrich); 1 % (vol/vol) B27 (Invitrogen, Life Technologies) and 6.2 g/l D-glucose.

435 Slices were incubated in a 5 % carbon dioxide (CO_2) humidified incubator at between 35 – 37 °C.
436 Recordings were made after 6-14 days in culture.
437 For human cortical acute brain slices, brain tissue from temporal cortex was obtained from adult
438 patients undergoing elective neurosurgical procedures at Mediclinic Constantiaberg Hospital to treat
439 refractory epilepsy (2 patients, 1 Male and 1 female, ages 28 and 41). Informed consent to use tissue
440 for research purposes was obtained from patients prior to surgery. Resected brain tissue was
441 transported from surgery to the laboratory in an ice-cold choline-based cutting solution composed of:
442 Choline Chloride (110 mM, Sigma-Aldrich), $NaHCO_3$ (26 mM, Sigma-Aldrich), D-glucose (10 mM, Sigma-
443 Aldrich), Sodium Ascorbate (11.6 mM, Sigma-Aldrich), $MgCl_2$ (7 mM, Sigma-Aldrich), Sodium Pyruvate
444 (3.1 mM, Sigma-Aldrich), KCl (2.5 mM, Sigma-Aldrich), NaH_2PO_4 (1.25 mM, Sigma-Aldrich) and $CaCl_2$
445 (0.5 mM, Sigma-Aldrich). Cutting solution was bubbled with carbogen gas (95% O_2, 5% CO_2) and had
446 an osmolality of approx. 300 mOsm. In the lab, the pia mater was carefully removed, and tissue was
447 trimmed into blocks for sectioning using a Compresstome (Model VF-210-0Z, Precisionary
448 Instruments). Slices were cut at 350 µm thickness and allowed to recover for ~30 min at 34 ºC in
449 standard aCSF composed of: NaCl (120 mM, Sigma-Aldrich), KCl (3 mM, Sigma-Aldrich), $MgCl_2$ (2 mM,
450 Sigma-Aldrich), $CaCl_2$ (2 mM, Sigma-Aldrich), NaH_2PO_4 (1.2 mM, Sigma-Aldrich), $NaHCO_3$ (23 mM,
451 Sigma-Aldrich) and D-Glucose (11 mM, Sigma-Aldrich). The aCSF was adjusted to pH 7.4 using 0.1 mM
452 NaOH (Sigma-Aldrich), was continuously carbogenated, and had an osmolality of ~300 mOsm. After
453 recovery, slices were left for at least 1 hr at room temperature before recording.
454

455 *Electrophysiology, calcium and glutamate imaging*

456 Brain slices were transferred to a submerged recording chamber on a patch-clamp rig, which was
457 maintained at a temperature between 28 and 30 °C and were continuously superfused with standard
458 aCSF bubbled with carbogen gas (95 % O_2: 5 % CO_2, supplier?) using peristaltic pumps (Watson-
459 Marlow). The standard aCSF was composed of: NaCl (120 mM, Sigma-Aldrich); KCl (3 mM, Sigma-

460 Aldrich); $MgCl_2$ (2 mM, Sigma-Aldrich); $CaCl_2$ (2 mM, Sigma-Aldrich); NaH_2PO_4 (1.2 mM, Sigma-Aldrich);
461 $NaHCO_3$ (23 mM, Sigma-Aldrich) and D-Glucose (11 mM, Sigma-Aldrich) in deionised water with pH
462 adjusted to between 7.35 and 7.40 using 0.1 mM NaOH (Sigma-Aldrich). Neurons in the CA3 region of
463 the hippocampus were visualized using a Zeiss Axioskop or Olympus BX51WI upright microscope using
464 20x or 40x water-immersion objectives and targeted for recording. Micropipettes were prepared (tip
465 resistance between 3 and 7 MΩ) from borosilicate glass capillaries (outer diameter 1.2 mm, inner
466 diameter 0.69 mm, Harvard Apparatus Ltd) using a horizontal puller (Sutter). Recordings were made
467 in current-clamp mode using Axopatch 200B amplifiers (Axon Instruments) and data acquired using
468 WinWCP (University of Strathclyde) or Igor (Markram Laboratory, Ecole polytechnique fédérale de
469 Lausanne). Matlab (MathWorks) was utilised for trace analysis. Two internal solutions were used: a
470 "standard" internal solution (K-gluconate (126 mM), KCl (4 mM), HEPES (10 mM) Na_2ATP (4 mM),
471 NaGTP (0.3 mM) and Na_2-phosphocreatine (10 mM); Sigma-Aldrich) and a "caesium" internal solution
472 (CsOH (120 mM), Gluconic acid (120 mM), HEPES (40 mM), Na_2ATP (2 mM), NaGTP (0.3 mM) and NaCl
473 (10 mM); Sigma-Aldrich). Experimental substances were puffed onto neurons using an OpenSpritzer,
474 a custom made pressure ejection system (46). Current was injected if required to ensure a neuronal
475 resting membrane potential within 2 mV of -60 mV. In all puffing experiments each data point
476 represents the mean peak puff-induced change in membrane potential from 10 sweeps. In some
477 experiments tetrodotoxin (TTX) (2 µM, Sigma-Aldrich) was added to the aCSF to block voltage-gated
478 sodium channels.
479 For calcium and glutamate imaging, organotypic hippocampal mouse brain slices were virally
480 transfected with a genetically-encoded Ca^{2+} reporter (GCAMP6s under the synapsin 1 gene promoter,
481 AAV1.Syn.GCaMP6s.WPRE.SV40, supplier?) or a genetically-encoded glutamate reporter (iGluSnFR
482 under the human synapsin 1 gene promoter, pAAV.hSynapsin.SF-iGluSnFR.A184S, supplier?) one day
483 post culture using the OpenSpritzer and imaged 5 days later using an Olympus BX51WI microscope,
484 20x water-immersion objective, CCD camera (CCE-B013-U, Mightex for the calcium imaging and an
485 Andor Zyla 4.2 for the glutamate imaging). For the calcium imaging excitation was provided using a

486 470 nm LED (Thorlabs). For glutamate imaging, excitation was generated using a LED-based light
487 engine, 475/28 nm (Lumencor). For both imaging paradigms a Chroma 39002 EGFP filter set (480/30
488 nm excitation filter, 505 nm dichroic, 535/40 nm emission filter) was utilised. Images were collected
489 using µManager (47). Calcium imaging data was analysed using Caltracer3 beta. Glutamate imaging
490 data was analysed using custom scripts written in Matlab.
491 For real-time imaging of glutamate signaling in neurons adjacent to a live *T. crassiceps* larva, mouse
492 hippocampal organotypic brain slices were virally transfected with a genetically-
493 encoded glutamate reporter (iGluSnFR under the human synapsin 1 promoter, pAAV.hSynapsin.SF-
494 iGluSnFR.A184S) one day post culture using the OpenSpritzer. Five to six days later a brain slice would
495 be removed from the culture insert by cutting a roughly 15 mm diameter circle of the membrane out,
496 with the brain slice located in the centre of the circle. The membrane was then placed in a glass-
497 bottomed petri dish containing a drop of aCSF, with the brain slice making contact with the glass
498 bottom. At this point, a single *T. crassiceps* larvae (harvested on the same day or one day prior) of
499 approximately 1 – 2 mm in length was inserted under the membrane with a pasteur pipette and
500 carefully maneuvered such until it was adjacent to one edge of the slice. A stainless-steel washer of
501 an appropriate size was then placed on top of the membrane such that it surrounded the brain slice
502 and larva, securing them in place. An additional 2 – 3 ml of carbogen-bubbled aCSF was then added
503 to the petri-dish. The petri-dish was placed in a small incubating chamber (37 °C, 5 % CO_2) in a LSM
504 880 airyscan confocal microscope (Carl Zeiss, ZEN SP 2 software). Glutamate signaling in the brain area
505 directly adjacent to the larvae was captured with a tile scan of the area every 90 sec for 15 min using
506 a 40x water-immersion lens (Zeiss) and a 488 nm laser (Zeiss). Transmitted light was also captured to
507 confirm presence and movement of the larva at the site of interest.
508
509 Pharmacological manipulations were performed by bath application of drugs using a perfusion system
510 (Watson-Marlow). Mecamylamine, Amiloride, D-AP5 and CNQX were purchased from Tocris.
511 Kynurenic acid and Substance P were acquired from Sigma-Aldrich.

Data analysis and statistics

Data was graphed and analysed using Matlab, ImageJ, Microsoft Excel and GraphPad Prism. All data was subjected to a Shapiro-Wilk test to determine whether it was normally distributed. Normally distributed populations were subjected to parametric statistical analyses, whilst skewed data was assessed using non-parametric statistical analyses. Parametric tests included: unpaired student's t-test; paired student's t-test; one-way analysis of variance (ANOVA) with Tukey's post hoc test and repeated measures ANOVA with Tukey's post-hoc test. Non-parametric tests included: Mann-Whitney test; Wilcoxin ranked pairs test; Kruskal Wallis one-way ANOVA with post hoc Dunn's Multiple Comparison test; and Friedman test with post-hoc Dunn's Multiple Comparison test. The confidence interval for all tests was set at 95%.

Acknowledgements

We would like to acknowledge Dr Philip Fortgens (Division of Chemical Pathology, Department of Pathology, University of Cape Town and National Health Laboratory Service (affiliation when the analyses were done) as well as Dr James T. Butler and Dr Roger Melvill of the Epilepsy Unit, Constantiaberg Mediclinic together with the anonymous patient who provided human cortical brain tissue. The research leading to these results has received funding from a Royal Society Newton Advanced Fellowship (NA140170) and a University of Cape Town Start-up Emerging Researcher Award to JVR and grant support from the Blue Brain Project, the National Research Foundation of South Africa, the FLAIR Fellowship Programme (FLR\R1\190829): a partnership between the African Academy of Sciences and the Royal Society funded by the UK Government's Global Challenges Research Fund, a Wellcome Trust Seed Award and a Wellcome Trust International Intermediate Fellowship (222968/Z/21/Z). KAS was supported by a European Commission Marie Sklodowska-Curie Global Fellowship (Grant 657638, WORMTUMORS). CS, UFP and CPdC were supported by the Federal Ministry of Education and Research of Germany (BMBF), Project title: "CYSTINET-Africa" (01KA1610, Germany II). The funders had no role in study design, data collection and analysis, decision to publish, or preparation of the manuscript.

Competing interests

The authors declare that there are no competing interests relevant to this manuscript.

References

1. Diop AG, Boer HM De, Mandlhate C, Prilipko L, Meinardi H. The global campaign against epilepsy in Africa. Acta Trop. 2003;87:149–59.
2. Preux PM, Druet-Cabanac M. Epidemiology and aetiology of epilepsy in sub-Saharan Africa. Lancet Neurol. 2005 Jan;4(1):21–31.
3. Trevisan C, Mkupasi EM, Ngowi HA, Forkman B, Johansen M V. Severe seizures in pigs naturally infected with Taenia solium in Tanzania. Vet Parasitol. 2016;220:67–71.

4. Garcia HH, Del OH. Antiparasitic treatment of neurocysticercosis - The effect of cyst destruction in seizure evolution. Epilepsy & Behavior. 2017;76:158–62.
5. Nash TE, Mahanty S, Garcia HH. Neurocysticercosis-More Than a Neglected Disease. PLoS Negl Trop Dis. 2013;7(4):7–9.
6. Ndimubanzi PC, Carabin H, Budke CM, Nguyen H, Qian YJ, Rainwater E, et al. A systematic review of the frequency of neurocyticercosis with a focus on people with epilepsy. PLoS Negl Trop Dis. 2010;4(11).
7. de Lange A, Mahanty S, Raimondo J v. Model systems for investigating disease processes in neurocysticercosis. Parasitology [Internet]. 2018 Nov 15;1–10. Available from: http://www.ncbi.nlm.nih.gov/pubmed/30430955
8. Garcia HH, Del OH. Antiparasitic treatment of neurocysticercosis - The effect of cyst destruction in seizure evolution. Epilepsy & Behavior. 2017;76:158–62.
9. Vezzani A, Fujinami RS, White HS, Preux P marie, Blümcke I, Sander JW, et al. Infections, inflammation and epilepsy. Acta Neuropathol. 2016;131:211–34.
10. Nash TE, Mahanty S, Loeb J a., Theodore WH, Friedman A, Sander JW, et al. Neurocysticercosis: A natural human model of epileptogenesis. Epilepsia. 2015 Feb;56(2):177–83.
11. Robinson P, Garza A, Weinstock J, Serpa J a, Goodman JC, Eckols KT, et al. Substance P causes seizures in neurocysticercosis. PLoS Pathog [Internet]. 2012 Feb [cited 2013 Sep 11];8(2):e1002489. Available from: http://www.pubmedcentral.nih.gov/articlerender.fcgi?artid=3276565&tool=pmcentrez&rendertype=abstract
12. Sun Y, Chauhan A, Sukumaran P, Sharma J, Singh BB, Mishra BB. Inhibition of store-operated calcium entry in microglia by helminth factors: implications for immune suppression in neurocysticercosis. J Neuroinflammation. 2014 Dec 24;11(1):210.
13. Vendelova E, Camargo de Lima J, Lorenzatto KR, Monteiro KM, Mueller T, Veepaschit J, et al. Proteomic Analysis of Excretory-Secretory Products of Mesocestoides corti Metacestodes Reveals Potential Suppressors of Dendritic Cell Functions. PLoS Negl Trop Dis. 2016;10(10):1–27.
14. Forman CJ, Tomes H, Mbobo B, Burman RJ, Jacobs M, Baden T, et al. Openspritzer: an open hardware pressure ejection system for reliably delivering picolitre volumes. Sci Rep. 2017 May;7(1):2188.
15. Bear MF, Connors BW, Paradiso MA. Neuroscience: Exploring the brain. Third. Lupash E, Connolly E, Dilernia B, Williams P, editors. Philadelphia, Baltimore, New York, London, Buenos Aires, Hong Kong, Sydney, Tokyo: Lippincott Williams & Wilkins; 2007.
16. Bear MF, Connors BW, Paradiso MA. Neuroscience: Exploring the brain. Third. Lupash E, Connolly E, Dilernia B, Williams P, editors. Philadelphia, Baltimore, New York, London, Buenos Aires, Hong Kong, Sydney, Tokyo: Lippincott Williams & Wilkins; 2007.
17. Dingledine R, McBain CJ. Glutamate and Aspartate Are the Major Excitatory Transmitters in the Brain. 1999;
18. Marvin JS, Borghuis BG, Tian L, Cichon J, Harnett MT, Akerboom J, et al. An optimized fluorescent probe for visualizing glutamate neurotransmission. Nat Methods. 2013 Feb;10(2):162–70.
19. Verastegui MR, Mejia A, Clark T, Gavidia CM, Mamani J, Ccopa F, et al. Novel Rat Model for Neurocysticercosis Using Taenia solium. Am J Pathol. 2015;185(8):2259–68.
20. Stringer JL, Marks LM, White AC, Robinson P. Epileptogenic activity of granulomas associated with murine cysticercosis. Exp Neurol. 2003 Oct;183(2):532–6.
21. Sun DA, Sombati S, DeLorenzo RJ. Glutamate Injury–Induced Epileptogenesis in Hippocampal Neurons. Stroke. 2001 Oct 1;32(10):2344–50.
22. Sombati S, Delorenzo RJ. Recurrent spontaneous seizure activity in hippocampal neuronal networks in culture. J Neurophysiol. 1995 Apr;73(4):1706–11.

601 23. DeLorenzo R, … SPP of the, 1998 undefined. Prolonged activation of the N-methyl-d-aspartate
602 receptor–Ca2+ transduction pathway causes spontaneous recurrent epileptiform discharges in
603 hippocampal neurons. National Acad Sciences.
604 24. Anderson WW, Anderson WW, Lewis D V., Scott Swartzwelder H, Wilson WA. Magnesium-free
605 medium activates seizure-like events in the rat hippocampal slice. Brain Res. 1986;398(1):215–
606 9.
607 25. Stasheff S, Anderson W, Clark S, Science WW, 1989 undefined. NMDA antagonists differentiate
608 epileptogenesis from seizure expression in an in vitro model. science.sciencemag.org.
609 26. Ziobro JM, Deshpande LS, DeLorenzo RJ. An organotypic hippocampal slice culture model of
610 excitotoxic injury induced spontaneous recurrent epileptiform discharges. Brain Res. 2011 Jan
611 31;1371:110–20.
612 27. Croucher MJ, Bradford HF. NMDA receptor blockade inhibits glutamate-induced kindling of the
613 rat amygdala. Brain Res. 1990;506(2):349–52.
614 28. Croucher MJ, Bradford HF, Sunter DC, Watkins JC. Inhibition of the development of electrical
615 kindling of the prepyriform cortex by daily focal injections of excitatory amino acid antagonists.
616 Eur J Pharmacol. 1988;152(1–2):29–38.
617 29. Rice AC, Delorenzo RJ. NMDA receptor activation during status epilepticus is required for the
618 development of epilepsy. Brain Res. 1998;782(1–2):240–7.
619 30. Hauser WA, Annegers JF, Kurland LT. Prevalence of Epilepsy in Rochester, Minnesota: 1940–
620 1980. Epilepsia. 1991 Aug;32(4):429–45.
621 31. Forsgren L, Beghi E, Oun A, Sillanpaa M. The epidemiology of epilepsy in Europe - a systematic
622 review. Eur J Neurol. 2005 Apr 1;12(4):245–53.
623 32. Ankarcrona M, Dypbukt JM, Bonfoco E, Zhivotovsky B, Orrenius S, Lipton SA, et al. Glutamate-
624 induced neuronal death: A succession of necrosis or apoptosis depending on mitochondrial
625 function. Neuron. 1995 Oct 1;15(4):961–73.
626 33. Lee HHC, Deeb TZ, Walker JA, Davies PA, Moss SJ. NMDA receptor activity downregulates KCC2
627 resulting in depolarizing GABAA receptor–mediated currents. Nat Neurosci. 2011 Jun
628 1;14(6):736–43.
629 34. Terunuma M, Vargas KJ, Wilkins ME, Ramírez OA, Jaureguiberry-Bravo M, Pangalos MN, et al.
630 Prolonged activation of NMDA receptors promotes dephosphorylation and alters
631 postendocytic sorting of GABAB receptors. Proceedings of the National Academy of Sciences.
632 2010 Aug 3;107(31):13918–23.
633 35. Buckingham SC, Campbell SL, Haas BR, Montana V, Robel S, Ogunrinu T, et al. Glutamate
634 release by primary brain tumors induces epileptic activity. Nat Med. 2011 Oct 11;17(10):1269–
635 74.
636 36. Santosh V, Sravya P. Glioma, glutamate (SLC7A11) and seizures-a commentary. Ann Transl
637 Med. 2017 May;5(10):214.
638 37. Sontheimer H. A role for glutamate in growth and invasion of primary brain tumors. J
639 Neurochem. 2008 Apr 1;105(2):287–95.
640 38. Takano T, Lin JHC, Arcuino G, Gao Q, Yang J, Nedergaard M. Glutamate release promotes
641 growth of malignant gliomas. Nat Med. 2001 Sep;7(9):1010–5.
642 39. Huang W, Choi W, Chen Y, Zhang Q, Deng H, He W, et al. A proposed role for glutamine in
643 cancer cell growth through acid resistance. Cell Res. 2013 May 29;23(5):724–7.
644 40. Adalid-Peralta L, Arce-Sillas A, Fragoso G, Cárdenas G, Rosetti M, Casanova-Hernández D, et al.
645 Cysticerci drive dendritic cells to promote in vitro and in vivo tregs differentiation. Clin Dev
646 Immunol. 2013;2013:1–9.
647 41. Verma A, Prasad KN, Cheekatla SS, Nyati KK, Paliwal VK, Gupta RK. Immune response in
648 symptomatic and asymptomatic neurocysticercosis. Med Microbiol Immunol. 2011 Nov
649 1;200(4):255–61.

42. Prodjinotho UF, Gres V, Henkel F, Lacorcia M, Dandl R, Haslbeck M, et al. Helminthic dehydrogenase drives PGE 2 and IL-10 production in monocytes to potentiate Treg induction . EMBO Rep. 2022 May 4;23(5).
43. Perea G, Araque A. GLIA modulates synaptic transmission. Brain Res Revs. 2010 May;63(1–2):93–102.
44. Seifert G, Carmignoto G. Astrocyte dysfunction in epilepsy. Brain Res Rev. 2010 May 1;63(1–2):212–21.
45. Stoppini L, Buchs PA, Muller D. A simple method for organotypic cultures of nervous tissue. J Neurosci Meth. 1991 Apr;37(2):173–182.
46. Forman CJ, Tomes H, Mbobo B, Baden T, Raimondo J V. Openspritzer: an open hardware pressure ejection system for reliably delivering picolitre volumes. bioRxiv. 2016;093633.
47. Edelstein A, Amodaj N, Hoover K, Vale R, Stuurman N. Computer Control of Microscopes Using µManager. In: Current Protocols in Molecular Biology. Hoboken, NJ, USA: John Wiley & Sons, Inc.; 2010. p. 14.20.1-14.20.17.